

Long-Range Coulomb Interaction in Bilayer Graphene

D. S. L. Abergel* and Tapash Chakraborty

Department of Physics and Astronomy, University of Manitoba, Winnipeg, Manitoba, R3T 2N2, Canada
(Received 1 October 2008; published 6 February 2009)

We report on our studies of interacting electrons in bilayer graphene in a magnetic field. We demonstrate that the long-range Coulomb interactions between electrons in this material are highly important and account for the band asymmetry in recent optical magneto-absorption experiments [E. A. Henriksen *et al.*, Phys. Rev. Lett. **100**, 087403 (2008)]. We show that in the unbiased bilayer (where both layers are at the same electrostatic potential), the interactions can cause mixing of Landau levels in moderate magnetic fields. For the biased bilayer (when the two layers are at different potentials), we demonstrate that the interactions are responsible for a change in the total spin of the ground state for half-filled Landau levels in the valence band.

DOI: 10.1103/PhysRevLett.102.056807

PACS numbers: 73.22.-f, 73.43.-f

Monolayer graphene is a two-dimensional hexagonal crystal of carbon atoms whose gapless, relativisticlike, linear low energy dispersion has made it the subject of intense study since it was first isolated in 2004 [1]. Bilayer graphene (BLG) [2], the subject of our present study, consists of a pair of monolayers bound by relatively weak dimer bonds formed perpendicular to the monolayer planes. Both the conduction and valence bands have low energy structure consisting of two quadratic branches separated by the energy associated with the dimer bond, γ_1 , and the lower conduction band and upper valence band are degenerate at the K points of the Brillouin zone. The existence of chiral charge carriers with a Berry's phase of 2π was confirmed by observation of the integer quantum Hall effect [3] where the low energy Landau level (LL) spectrum is approximately linear in the field with $E_{n\pm} \approx \pm \hbar\omega_c \sqrt{n(n-1)}$ for $n \geq 0$ where ω_c is the cyclotron frequency, and the spectrum includes a doubly degenerate LL at zero energy [4]. It has been predicted theoretically [4–6] and observed experimentally [7,8], that a gap can be induced in the low energy band structure by breaking the symmetry between the two layers. Switching of the conduction current by sweeping the Fermi energy through the gapped region has been observed at low temperatures [9], and this has led to a surge of interest in gapped BLG.

While the single-particle theory of BLG is well known [2,4–6], it has been shown that the electron-electron interactions are significant in monolayer graphene [10,11]. The Coulomb interaction (CI) has been studied in the ungapped bilayer [12], while the biasing potential was considered in the context of a ferromagnetic transition due to short-range interactions in the mean-field approximation at zero magnetic field [13], and the absence of a contribution to the intra-LL cyclotron resonance from the electron interactions has been predicted within Hartree-Fock theory [14]. However, the effect of the long-range CI on the ground state of the biased system in a magnetic field has not been

investigated, and we address this problem in the current Letter.

We find that the long-range nature of the CI makes significant changes to the properties of the low energy charge carriers for BLG in a magnetic field. The interactions are significantly stronger for electrons in the lowest LL, and this manifests itself in an observable way by lifting the degeneracy of the cyclotron resonance transitions at filling factors ± 4 [15,16]. It also allows the possibility of mixing of the LLs which were well separated in energy when the CIs were not considered. By calculating the explicit form of the ground state wave function, we show how this mixing fundamentally changes the nature of the ground state in the biased bilayer, by inducing a finite spin polarization for half-filled LLs.

We model BLG as two sheets, each containing two inequivalent triangular sublattices (labeled A and B) of carbon atoms. In the Bernal stacking arrangement, the interlayer bonds consist of dimers formed from atomic orbitals associated with the A sublattice in one layer and the B sublattice in the other (see Fig. 1), and the energy associated with this bond is denoted γ_1 [17]. We allow for a static electric potential U to be applied between the layers,

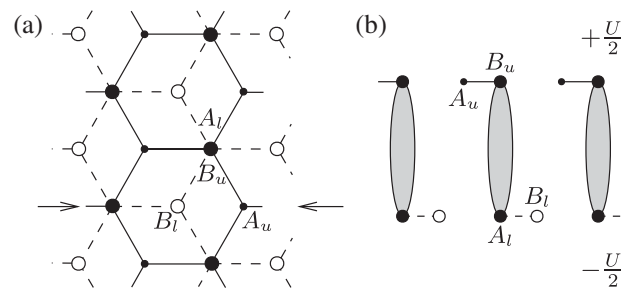


FIG. 1. The lattice structure of bilayer graphene. The upper (lower) lattice is shown by solid (dashed) lines. (a) The top-down view; (b) the side-on view projected along the axis between the two arrows in (a).

so that the upper (lower) layer has potential $U/2$ ($-U/2$). In a strong magnetic field we can write the tight-binding Hamiltonian using a four component single valley basis where $\xi = \pm 1$ labels the valley [4] as

$$\mathcal{H}_0 = \begin{pmatrix} \frac{\xi U}{2} & 0 & 0 & \xi v_F \pi^\dagger \\ 0 & -\frac{\xi U}{2} & \xi v_F \pi & 0 \\ 0 & \xi v_F \pi^\dagger & -\frac{\xi U}{2} & \gamma_1 \\ \xi v_F \pi & 0 & \gamma_1 & \frac{\xi U}{2} \end{pmatrix}, \quad (1)$$

where π and π^\dagger are the operators corresponding to electron hops between neighboring atoms (in opposite sublattices in the same layer). The spectrum ε_n^ξ is found from the quartic polynomial [6] derived from the Schrödinger equation associated with the Hamiltonian in Eq. (1), where $n \in \{0, 1, 2, \dots\}$. Additionally, we denote the band of a particular LL by placing a “+” (“−”) after the level index for the conduction (valence) band. The wave functions associated with the LLs from the two low energy bands are given by

$$\psi_{n\pm}^\xi = e^{iky} (a_{n\pm}^\xi \varphi_{n+1}, b_{n\pm}^\xi \varphi_{n-1}, c_{n\pm}^\xi \varphi_n, d_{n\pm}^\xi \varphi_n)^T, \quad (2)$$

where the functions φ_n are the magnetic oscillator functions in the Landau gauge, and the coefficients a , b , c , and d are defined so that the overall wave function is normalized to unity. There are also levels with $n = 0 \pm$, which have wave functions $\psi_{0+}^K = e^{iky}(\varphi_0, 0, 0, 0)$, and $\psi_{0-}^{K'} = e^{iky}(\varphi_0, 0, 0, 0)$ with $\varepsilon = \pm \delta$; and $\psi_{0+}^{K'}$ and ψ_{0-}^K are defined as higher LLs above with the appropriate substitutions for n and ξ . When $U = 0$, these four states are degenerate yielding the eightfold degeneracy (including the factor of 2 for spin) seen in the integer quantum Hall effect in BLG [3]. We include the fermionic properties of the electrons by constructing Slater determinants for the noninteracting many body basis wave functions.

To include the effects of the long-range CI we consider the Hamiltonian $\mathcal{H}_{\text{Coul}} = \frac{1}{2} \sum_{i \neq j} \frac{e^2}{\epsilon |\vec{r}_i - \vec{r}_j|}$ where the vectors $\vec{r}_{i,j}$ label the positions of the electrons, and $\epsilon = 4\pi\epsilon_0\kappa$ is the dielectric constant of graphene. For graphene mounted on an SiO₂ substrate, $\kappa = 2.5$ [18]. Our analysis is conducted by employing the exact diagonalization scheme [19] in which we calculate the linear combination of noninteracting basis states which gives the ground state of the Hamiltonian $\mathcal{H} = \mathcal{H}_0 + \mathcal{H}_{\text{Coul}}$. This method entails dividing the infinite sheet into rectangular cells of dimension $L_x \times L_y$ [20] and applying periodic boundary conditions to the wave functions at the edges of each cell. The matrix elements of the interaction over the single-particle states are evaluated exactly, and the interaction between the cells is taken into account by adding the Madelung energy of a charged lattice [21].

The single-particle states included in the Hilbert space from which the noninteracting many body basis is constructed are as follows. There are four quantum numbers: The LL index n , the valley ξ , the spin, and the momentum $k = \pi m/L_x$. The values of the momentum are fixed when the boundary conditions are applied to the cell, and are

labeled by $0 \leq m \leq M - 1$ with $M = L_x L_y / (2\pi\lambda_B^2)$. The LLs selected are governed by the details of the system we wish to model, and M is set by computational restraints. Our model includes all interelectron screening effects since we calculate the exact matrix elements of the full Coulomb interaction, and it is well known that filled Landau levels with energy significantly below the Fermi level do not make additional contributions.

In order to reduce the size of the many body system (and so improve the calculation speed), we see that the Hamiltonian conserves the total momentum $\mu = \sum_{i=1}^N m_i \bmod M$. Therefore, we can perform a separate diagonalization for each value of μ , and reduce the basis size to approximately the $1/M$ th part. We define $S = \sum_i S_i$ to be the total spin of the many electron system, and since there is no spin-dependent term in the Hamiltonian, S_z (the projection of S on the z axis) is a good quantum number. Therefore we fix S_z to its minimum value while still being able to recover all eigenstates of S^2 [11], further reducing the many body basis size.

We consider two cases: First we demonstrate the strength of the interaction by calculating the shift in the energy of each LL due to interactions for $U = 0$ (an unbiased bilayer) and apply the results to recent experimental data. Then we examine the system where the filling factor is negative, the interlayer potential sizable, and the magnetic field strong. In this case, we observe changes in the total spin of the ground state as a function of U and the magnetic field strength B .

We model the unbiased bilayer near half-filling by taking a single-particle Hilbert space consisting of the $0+$ and $0-$ LLs with all possible spin and valley states at $U = 0$. Each integer value of the filling factor ν is simulated by taking the number of electrons $N = (\nu + 4)M$, and we have $M = 3$. Table I, part (a) shows the results of diagonalizing the resulting many body Hamiltonian and evaluating the energy change from the noninteracting ground state for integer filling factors. We see that the energy shift per electron reduces slightly as the LL fills.

In Table I, part (b), we show the energy shift due to the CI for electrons in higher LLs (i.e., for levels with $|n| \geq 1$).

TABLE I. Energy shift per electron due to the Coulomb interaction for integer filling factors in the (a) $0\pm$ LL and (b) $|n| \geq 1$ LLs, for $U = 0$. Energy units are $e^2/(\epsilon\lambda_B)$, the number of momentum states $M = 3$, and the magnetic field $B = 3$ T.

(a) Filling factor	−3	−2	−1	0
Energy shift	−0.6443	−0.6443	−0.6443	−0.6443
Filling factor	1	2	3	4
Energy shift	−0.6316	−0.6222	−0.6148	−0.6085
(b) Landau level n	1+	2+	3+	4+
$\nu_n = 1$	−0.4766	−0.5001	−0.5242	−0.5160
$\nu_n = 2$	−0.4705	−0.4880	−0.5176	−0.5110
$\nu_n = 3$	−0.4645	−0.4759	−0.5111	−0.5061
$\nu_n = 4$	−0.4584	−0.4638	−0.5046	−0.5012

We have taken a single-particle Hilbert space consisting of all spin and valley states within one LL. The filling factor ν_n within LL n can range between 0 (corresponding to an empty level) and 4 (a filled level), so that $\nu_n = 4$ and $\nu_{n+1} = 0$ describe the same overall filling factor. The number of electrons is set by $N = \nu_n M$, and in order to allow direct comparison with the lowest LL we restrict ourselves to $M = 3$. The energy associated with the interaction of electrons is very similar in each of the higher LLs, and that the interaction energy per particle is slightly reduced as the LL is filled. We have verified that the results are identical in the valence band.

Together, Table I, parts (a) and (b), show that the effect of the long-range CIs is considerable, and that for this value of the magnetic field ($B = 3$ T) the shift in the higher LLs is only about two-thirds that of the lowest LL. This difference in the shift will reveal itself in the infrared absorption spectrum of bilayer graphene, since the energy of the optical transitions depends entirely on the direct energy spacing between levels. At $U = 0$ and $\nu = -4$, the lowest energy transition is from the $1-$ level to the $0\pm$ level, while at $\nu = +4$ the lowest energy transition is from $0\pm$ to $1+$. Therefore, if the $0\pm$ is shifted with respect to the two $|n| = 1$ levels, the degeneracy of these two transitions predicted in the single-particle theory [16] will be lifted. In Fig. 2 we show the predictions of our theory in comparison to recent experimental data [15]. Panes (a) and (b) show comparison of the valence band transitions (i.e., for $\nu = -4$) for two values of γ_1 and three values of ν_F . The energy of the excited state is calculated as the sum of the full interacting energy of $N - 1$ electrons in the $1-$ level and one electron in the $0\pm$ level (where we assume no LL mixing because the magnetic field is strong). The transition energy is the difference between this and the energy of N interacting electrons in the $1-$ level. Pane (c) shows the comparison of theoretical and experimental data in both bands for the best values of parameters. The correspondence to our theory is clear.

In Fig. 3 we show the energy shift and absolute energy of filled LLs as a function of the magnetic field. The strength

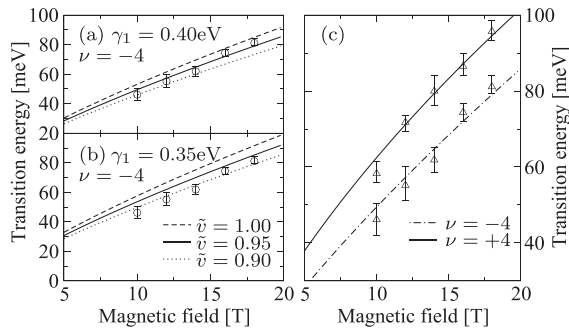


FIG. 2. Electron-hole asymmetry in the inter-LL optical transition energy. The experimental data (represented as points) are taken from Ref. [15], Fig. 2. In (a) and (b), $\tilde{\nu} = \nu_F / (10^6 \text{ ms}^{-1})$; in (c) we take $\gamma_1 = 0.4$ eV, $\nu_F = 0.95 \times 10^6 \text{ ms}^{-1}$; $M = 6$ throughout.

of the interaction scales with $e^2 / (\epsilon \lambda_B) \propto \sqrt{B}$ with a roughly constant coefficient, while the LL spacing goes as $\hbar \omega_c \propto B$, so for lower values of the field, the $n = 0\pm$ level crosses the $2-$ and $1-$ levels as shown in Fig. 3(b). The data shown here were calculated with $\kappa = 2.5$, modeling graphene [18] deposited on an SiO_2 substrate. For suspended graphene (where $\kappa \approx 1$), it is conceivable that the effect of the interaction would be even stronger. Additionally, the effect of the interlayer potential is to bring together the valence band LLs with low index [6], so it is plausible that the interactions will cause significant mixing between these levels.

Now we turn our attention to the system with an interlayer potential applied, so that $U \neq 0$. With a finite gap between the $0+$ and $0-$ levels and nonzero filling factor, it is possible to consider the negatively doped system by taking only those single-particle states which are in the valence band. Therefore we select the single-particle states which form the Slater determinants describing the non-interacting basis states by taking all spin and valley states of the $0-$ and $1-$ LLs. We have $M = 2$ and the number of electrons is related to the filling factor by $N = (\nu + 8)M$. Diagonalizing this system for half-filled LLs (so for $\nu = -6$ and $\nu = -2$), and calculating the expectation value of the total spin operator S^2 over the resulting ground state as a function of the magnetic field and the interlayer bias gives the data shown in the plots in Figs. 4(a) and 4(b). We have superimposed lines which represent the energy at which the single-particle energy levels cross, as labeled in the legend. We have also calculated the expectation of the total valley quantum number for each of these systems and find that it is constant with a value equal to 2. This is expected for half-filled LLs because of the lifting of the valley degeneracy in the single-particle theory by the interlayer potential [5,6]. The plots show that there is an abrupt change in the total spin of the ground state, and a range of parameters where there is a nonzero polarization of the spin. This transition is not directly related to the crossings of the single-particle states, since the position and slope of the transitions do not match the corresponding

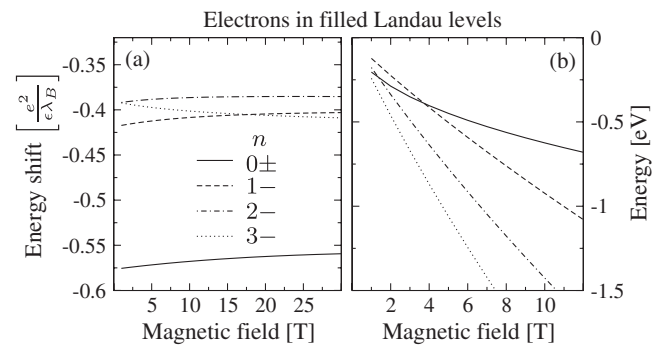


FIG. 3. (a) The energy shift per electron of filled LLs. (b) The absolute energy per electron of filled LLs showing the crossing between the $n = 0\pm$ degenerate level and the higher LLs in the valence band. In both plots $U = 0$, and $M = 5$.

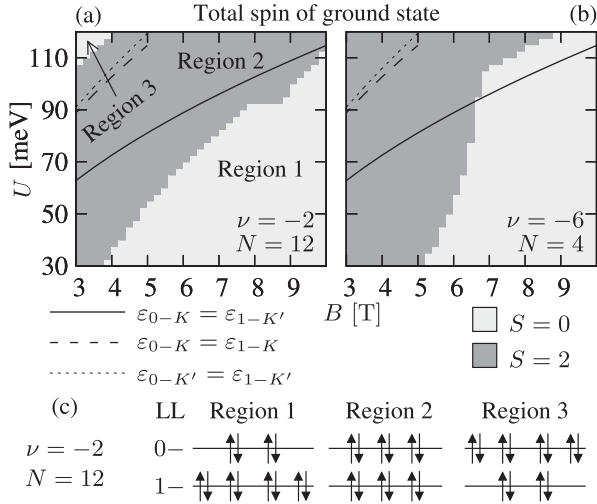


FIG. 4. The total spin of the ground state of the (a) $\nu = -2$ and (b) $\nu = -6$ systems. $M = 2$ and $N = (\nu + 8)M$. The lines show the crossing points of the single-particle states. The graining is due to the finite interval between data points. (c) The occupancy of the single electron states in the interacting many body ground state for each region of the plot in (a). The z projection of the total spin is fixed at zero as described in the text.

lines superimposed on the plots. This effect is therefore purely due to the CI, and, in particular, to the exchange contribution which minimizes the energy of spin-polarized many body states.

Figure 4(c) shows the occupation of the single-particle levels in the interacting many body ground state of the $\nu = -2$ system. For simplicity, we display only the LL index of the states. The actual ground state is a coherent combination of several noninteracting basis states, where the combination of LL indices is consistent but different arrangements of momentum and valley states each come with identical prefactors in the linear combination. In the lower-right region of the parameter space, the electrons occupy as many of the $1-$ states as possible. Moving toward the upper-left region, the $0-$ levels become successively more populated. The absence of spin polarization in regions 1 and 3 is caused by the pairing of electrons in the same valley. In region two, where there are six electrons per LL, this pairing is incomplete and the spin polarization finite. The pattern of filling in the two regions of the $\nu = -6$ system is identical.

From an experimental point of view, it is well known that it is possible to separate the effect of the orbital magnetization from that due to the spin polarization by tilting the magnetic field. In the quantum Hall regime, transitions in the ground state total spin have been observed by measurement of the magnetoresistance, notably by spikes associated with the change of state [22], and also as reentrant behavior as a function of the tilt angle relative to the magnetic field [23]. These methods may also be relevant in the case we discuss. Additionally, in the case of

bilayer graphene, the orbital effects can be kept fixed by keeping B constant and tuning U across the phase transition (see Fig. 4).

In conclusion, we have shown that the long-range CI between electrons plays an important role near the Dirac point in BLG. In the unbiased case, the interactions will cause a change in the cyclotron resonance energies associated with the $0\pm$ LL, and LL mixing between the $0\pm$ and $1-$ levels is induced for moderate magnetic fields. If an interlayer bias is applied to split the valence and conduction bands, the electron-electron interactions precipitate a transition in the total spin of the ground state of half-filled LLs for certain ranges of parameters. These effects will have fundamental implications for the design of devices made from bilayer graphene.

We acknowledge useful discussions with Yuanbo Zhang (Berkeley), and financial support from the Canada Research Chairs Program and the NSERC Discovery Grant.

*abergel@cc.umanitoba.ca

- [1] K. S. Novoselov *et al.*, Science **306**, 666 (2004); A. K. Geim and K. S. Novoselov, Nature Mater. **6**, 183 (2007).
- [2] E. McCann, D. S. L. Abergel, and V. I. Fal'ko, Solid State Commun. **143**, 110 (2007).
- [3] K. S. Novoselov *et al.*, Nature Phys. **2**, 177 (2006).
- [4] E. McCann and V. I. Fal'ko, Phys. Rev. Lett. **96**, 086805 (2006).
- [5] E. McCann, Phys. Rev. B **74**, 161403(R) (2006).
- [6] J. M. Pereira, Jr., F. M. Peeters, and P. Vasilopoulos, Phys. Rev. B **76**, 115419 (2007).
- [7] T. Ohta *et al.*, Science **313**, 951 (2006).
- [8] E. V. Castro *et al.*, Phys. Rev. Lett. **99**, 216802 (2007).
- [9] J. B. Oostinga *et al.*, Nature Mater. **7**, 151 (2008).
- [10] A. Iyengar *et al.*, Phys. Rev. B **75**, 125430 (2007).
- [11] T. Chakraborty and P. Pietiläinen, Europhys. Lett. **80**, 37007 (2007).
- [12] J. Nilsson *et al.*, Phys. Rev. B **73**, 214418 (2006).
- [13] E. V. Castro *et al.*, Phys. Rev. Lett. **100**, 186803 (2008).
- [14] Y. Barlas *et al.*, Phys. Rev. Lett. **101**, 097601 (2008).
- [15] E. A. Henriksen *et al.*, Phys. Rev. Lett. **100**, 087403 (2008).
- [16] D. S. L. Abergel and V. I. Fal'ko, Phys. Rev. B **75**, 155430 (2007).
- [17] We do not consider the effect of direct $A_n \leftrightarrow B_l$ hops, parametrized by $\gamma_3 \approx 0.3$ eV, since this does not lead to any additional states being coupled by the CI, so will not make any qualitative changes to the physics we describe.
- [18] T. Ando, J. Phys. Soc. Jpn. **75**, 074716 (2006).
- [19] For details, see T. Chakraborty and P. Pietiläinen, *The Quantum Hall Effects* (Springer-Verlag, Berlin, 1995), 2nd ed., pp. 41–3.
- [20] Throughout, we assume that $L_x = L_y$.
- [21] C. Kittel, *Introduction to Solid State Physics* (Wiley, Hoboken NJ, 2005), 8th ed., pp. 63–64.
- [22] E. P. De Poortere *et al.*, Science **290**, 1546 (2000).
- [23] J. P. Eisenstein *et al.*, Phys. Rev. Lett. **62**, 1540 (1989); R. G. Clark *et al.*, *ibid.* **62**, 1536 (1989).